PHYSICAL REVIEW E **66**, 011707 (2002)

Ordering transitions, biaxiality, and demixing in the symmetric binary mixture of rod and plate molecules described with the Onsager theory

Szabolcs Varga,* Amparo Galindo, and George Jackson
Department of Chemical Engineering and Chemical Technology, Imperial College of Science, Technology and Medicine, Prince Consort Road, London SW7 2BY, United Kingdom

(Received 14 January 2002; published 29 July 2002)

The phase behavior of a liquid-crystal forming binary mixture of generic hard rodlike and platelike particles is studied with the theory of Onsager [L. Onsager, Ann. N. Y. Acad. Sci. **51**, 627 (1949)] for nematic ordering. The mixture is chosen to be symmetric at the level of the second virial theory, so that the phase behavior of the two pure components is identical. A parameter q is used to quantify the effect of the unlike rod-plate excluded volumes on the phase behavior; a value of $q>1$ indicates that the unlike excluded volume is greater than the like excluded volume between the rods or plates, and a value of $q<1$ corresponds to a smaller unlike excluded volume. Two methods are used to solve the excluded volume integrals: the approximate L2 model [A. Stroobants and H. N. W. Lekkerkerker, J. Phys. Chem. **88**, 3669 (1984)], in which a second-order Legendre polynomial is used; and a numerical method where the integrals are solved exactly. By varying the unlike excluded volume interaction q, the isotropic phase is seen to be stabilized (small q) or destabilized (large q) with respect to the nematic phase for both models. Isotropic-isotropic demixing is also observed for the largest values of q due to the unfavorable contribution of the unlike excluded volume to the entropy of the system. A second-order nematic–biaxial nematic phase transition is observed for small values of q in the L2 approximation, and for all q in the exact calculation; in the latter case the stability of the biaxial phase is enhanced by increasing q, while in the L2 approximation nematic-nematic phase separation is favored. This result is the most striking difference between the two methods, and is in contrast with the results of previous studies. We show that the accuracy of the L2 expansion is particularly poor for parallel and perpendicular particle orientations.

DOI: 10.1103/PhysRevE.66.011707 PACS number(s): 64.70.Md, 64.60.Cn, 61.30.Cz

I. INTRODUCTION

One of the most striking developments in the field of liquid crystals was the seminal work of Onsager [1] presented in the 1940s. He predicted a transition from an orientationally disordered isotropic phase to an orientationally ordered uniaxial nematic phase in a fluid of infinitely thin rod particles with purely repulsive interactions. Using computer simulations, Vieillard-Baron [2] was the first to demonstrate the isotropic-nematic transition in a fluid of hard ellipses of finite length. Positionally ordered phases, such as smectic, columnar, and solid phases, were later also observed in systems of hard spherocylinders [3] and hard platelets [4]. Uniaxial nematic, smectic, columnar, and of course solid phases, are commonly observed experimentally [5]; in addition to the common uniaxial nematic phase, a so-called biaxial nematic phase has also been proposed. A biaxial nematic phase is positionally disordered (a characteristic of nematic phases), but exhibits orientational order in two, typically normal, directions. Such a fluid has been observed in computer simulations of hard biaxial particles [6], but has not, as yet, been confirmed experimentally. Extreme anisotropic ordering can also result in cubatic phases, which have been observed in fluids of hard platelike particles [7] and of hard cylinders [8].

It is therefore clear that attractive interactions are not necessary for the formation of liquid crystalline phases. Onsager already showed in his seminal work that the isotropic-nematic phase transition can be described in terms of purely entropic considerations. In order to maximize the total entropy, a competition arises between the orientational entropy (which favors the orientationally disordered state), and the available free volume (which increases the translational entropy and favors the orientationally ordered state) in the system. At high density the translational term becomes more important, favoring the formation of aligned phases in which the average excluded volume between particles is reduced. As the density is increased in a fluid of hard anisotropic particles, phase transitions from isotropic liquid to nematic, and more ordered, phases can be observed. In this work we are particularly interested in investigating the stability of the biaxial nematic phase, but instead of studying a fluid of hard-biaxial particles, we consider a binary mixture of uniaxial hard particles.

In mixtures of anisotropic molecules, an interplay between the orientational and free volume entropic contributions, and the ideal entropy of mixing, which is at a maximum for fully mixed states, gives rise to a very rich phase behavior; this is especially true when the components are of markedly different symmetry (such as rods and plates). Even in mixtures of components of the same symmetry (mixtures of thick and thin rods, for example), demixing can be observed if the gain in the free volume entropy overcomes the loss in the mixing and orientational entropy.

A complete theoretical study of mixtures of fluids of different symmetry is rather difficult due to the complex nature

---

*Corresponding author. Email address: s.varga@ic.ac.uk of the unlike interactions which give rise to computational difficulties. Lattice models [9–12] and Mayer-Saupe-type interaction potentials [13–15] are frequently used in order to simplify the numerical problem. The predictive ability of these approaches is rather limited, but they nevertheless provide a first insight of the qualitative phase behavior that could be expected in the experimental systems.

More recently, extensions of the original theory of Onsager have also been used to study the phase behavior in liquid crystalline mixtures of hard particles. Nematic-nematic phase separation has been obtained with extensions of the Onsager theory in mixtures of rods of different length [16–18], in mixtures of rods of different diameter [19], and in the so-called symmetric mixture of rods (a mixture of rods of different diameter and length but of the same like excluded volume) [20]. Surprisingly, isotropic-isotropic demixing is only observed in these mixtures when the rods are of different diameter, i.e., in a mixture of thick and thin rods [21] and in the symmetric mixture of rods. In these cases a four-phase coexistence point may exist in the phase diagram, as calculated by Sear and Mulder [20] for the symmetric mixture. In two recent studies, Hemmer [22,23] has studied the regions representing the demixing transitions both in the isotropic and the nematic phases for this mixture in terms of the molecular diameter and length ratios.

Much attention has also been paid to mixtures of rodlike and platelike molecules in recent years due to the combined interest in phase separation and phase biaxiality that may be exhibited by these systems. Considering that most liquid-crystal-forming molecules are biaxial in shape, it may at first be surprising to realize that biaxial nematic phases (nematic phases exhibiting alignment along the long molecular axis as well as in the direction of the molecular plane) are very rarely observed; it turns out that solidification preempts the existence of the biaxial phase in most cases. It may be more fruitful to investigate biaxial nematic phases in the context of mixtures of rod and plate molecules, as the composition offers an extra tunable variable and transitions to solid phases are normally destabilized in mixtures. Such a mixture was first studied by Alben [9] using a lattice mean-field model. Alben predicted the existence of a rod-plate biaxial nematic phase between a rod-rich uniaxial nematic phase and a plate-rich uniaxial nematic (discotic) phase, and the phase transitions from the uniaxial nematic to the biaxial nematic were found to be second order (i.e., continuous). The phase diagram predicted by Alben in 1973, was later confirmed for a lattice model including long-range isotropic (dispersion) interactions [24], as well as in off-lattice models using the Onsager [25] and Mayer-Saupe theories [15,26]. A number of recent studies of the phase behavior in mixtures of biaxial rod and plate molecules including association [27,28], and van der Waals like attractive interactions [29], have also been presented.

Discotic phases were observed experimentally a few years after the theoretical work of Alben, but the biaxial nematic phase still eludes experimental observation. Goozner and Labes [30] have studied a mixture of plate molecules "doped" with a small amount of rod molecules, and Hardouin *et al.* [31] a mixture of rod particles doped with a small amount of plate particles. These studies suggest that the ordered phases are destabilized on mixing. Yu and Saupe [32] have reported the phase diagram of a mixture of potassium laurate, 1-decanol, and water, and have found a biaxial nematic phase between two uniaxial phases (a micellar phase of bilayer structure, and a cylindrical micellar phase). Unfortunately, it has not since been possible to confirm this phase behavior. Van der Kooij and Lekkerkerker [33,34] have used essentially hard rod and plate colloidal particles to study the phase behavior of the mixtures. In their work the rods have an aspect ratio of about 10, and the plates of about 1/15; this means that the mixture is strongly asymmetric, as the excluded volume of the plate is much larger than that of the rod. Studying an extensive range of concentrations, they observe nematic-nematic demixing as well as nematic-columnar demixing, but never encounter a biaxial phase. Wensink *et al.* [35] have also studied this mixture in the context of the theory of Onsager incorporating the higher virial terms with the scaling approach of Parsons [36,37], finding good qualitative agreement with the experimental results.

A limited number of simulation studies have also been carried out which involve mixtures of rodlike and platelike molecules. Camp and Allen [38] studied mixtures of hard ellipsoidal particles of rod and plate shape with aspect ratios of 10 and 1/10, respectively. In this system nematic-nematic demixing appears to preempt the stable biaxial nematic phase. In an extension of the work Camp *et al.* [39] used the Gibbs ensemble simulation technique to study mixtures of hard ellipsoidal particles of aspect ratios 15 (rodlike) and 1/15 (platelike), and 20 and 1/20. In both mixtures, stable biaxial nematic phases were found to be in coexistence with a plate-rich nematic phase. A mixture of hard spherocylinders of aspect ratio 6, and hard cut spheres of aspect ratio 0.12 has also recently been studied using *NVT* Monte Carlo simulations [40]. In this case a demixing into a rod-rich nematic phase and plate-rich columnar phase is observed, together with a marked stabilization of the isotropic phase [40]; a biaxial phase was not found.

The range of stability of the biaxial nematic phase is still unresolved, because only limited regions of the molecular parameter space have been examined for each system. Even for a prescribed set of molecular parameters, a number of approximations have to be taken in order to solve the free energy expressions within a given theoretical description; these approximations can have a dramatic effect on the global phase diagram and on the stability of the biaxial phase in particular, as will be shown later in this work. Using the theory of Onsager to describe the continuous (off-lattice) rod-plate mixture, Stroobants and Lekkerkerker [25] solved the system of Euler-Lagrange integral equations with an approximate expression for the excluded volumes (the spherical harmonic expansion of the excluded volume was truncated at second order; see Sec. II). They observed a stable first-order isotropic-nematic transition and a second-order uniaxial–biaxial nematic transition. The two transitions meet at an equimolar composition, where the isotropic, uniaxial nematic, and biaxial nematic phases are in coexistence. It should be noted that their study was restricted to the case in which the rod-rod and plate-plate isotropic virial coefficients, as well as the unlike rod-plate isotropic virial coefficient are the same. More recently, Chrzanowska [41] has performed a more systematic study of the phase behavior in a mixture of hard rod and plate molecules considering two unlike excluded volumes that are taken to be different from those of the pure components. The study was limited, however, to a bifurcation analysis, which gives the upper bound for the stability of the less ordered phase, but which does not give conclusive information about the nature of the phase coexistence. The possibility of isotropic-isotropic or nematic-nematic demixing was not investigated, both of which could preempt the isotropic-nematic transition or the uniaxial–biaxial nematic transition; thus it is possible that the biaxial nematic phase is not stable in this system. One should also point out that the existing theoretical studies correspond only to a small portion of the global phase diagram within the Onsager approach for such mixtures; as indicated by Chrzanowska, different unlike excluded volume contributions give rise to very different types of phase behavior.

Van Roij and Mulder [10] used the Zwanzig model [42] to study the phase behavior of a mixture of rectangular rodlike and platelike blocks, examining a range of molecular parameters. For moderate aspect ratios they find strikingly different results from those of Stroobants and Lekkerkeker [25], and of Chrzanowska [41] as to the existence of a stable biaxial nematic phase. They were able to show that the stability of the biaxial nematic phase and its extent are very sensitive to the choice of the molecular aspect ratios. For moderately long and flat particles, no biaxial nematic phase is observed, while for longer and flatter particles this phase becomes more stable. A drawback of this study is that the orientational entropy term and the second virial term are rather poorly represented by the Zwanzig model. The aim of our work is to carry out a similar global investigation, concentrating on the effect of the unlike excluded volume on the phase behavior using the more accurate continuous theory of Onsager for rod-plate mixtures.

We undertake a comprehensive study of the phase coexistence in a symmetric mixture (equal pure component excluded volumes) of hard rod and plate particles, in order to give some insight into the phase behavior of rod-plate binary mixtures by studying different unlike excluded volume interactions between the rods and plates. We use the Gibbs free energy to confirm the stability of the phases relative to each other, including the possibility of demixing transitions in the isotropic and nematic phases. The isotropic, uniaxial nematic and the biaxial nematic phases are considered in detail. Additionally, particular attention is paid to the commonly used approximation for the description of the excluded volume interactions in which a second-order Legendre polynomial expansion is used (the L2 approximation). This approximation substantially reduces the computational burden, but results in a considerable error in the description of the excluded volumes especially for the parallel and perpendicular configurations. We study the effect of this inadequacy by comparing the phase behavior obtained using the L2 approximation with calculations in which the excluded volume integrals are solved numerically, i.e., without approximations.

This paper is organized as follows. A short description of Onsager's theory for ordering phase transitions in the specific case of binary mixtures of rod and plate molecules is given in the following section. The expressions for the equilibrium orientational distribution functions within the L2 description and for the full numerical description are presented in Sec. II A and II B. In Sec. II C a general (binodal and spinodal) demixing analysis is presented, and a simple analytical equation is derived for the isotropic-isotropic demixing transition curve. The phase diagrams for a number of mixtures with different length and diameter ratios, which are quantified through a parameter q that characterizes the unlike excluded volume interaction, are presented in Sec. IV, and we make some general conclusions in Sec. V.

II. THEORY

In this work we consider a binary mixture of hard uniaxial rodlike and platelike molecules, and study the fluid phase behavior of the system. We take into account isotropic, and orientationally ordered (nematic) phases, but not positionally ordered (smectic and solid) phases. In a binary mixture of uniaxial particles, which could be orientationally inhomogeneous but which is always spatially homogeneous, the positionally averaged density $\rho(\boldsymbol{\omega})$ is determined by an orientational distribution function $f(\boldsymbol{\omega})$ and the total number density ρ, so that it can be written as $\rho(\boldsymbol{\omega})=\rho f(\boldsymbol{\omega})$, where $\boldsymbol{\omega}$ is the orientational unit vector. In turn, the free energy F can be written as a sum of ideal and residual contributions given by

$$\frac{\beta F}{N}=\ln\rho-1+\sum_{i=1}^{2} x_i(\ln x_i+\sigma[f_i])+\rho B_2, \tag{1}$$

where $\beta=1/kT$ (T is the temperature and k is Boltzmann's constant), $\rho=N/V$ is the number density, x_i is the mole fraction of component i, and $\boldsymbol{\omega}$ is the orientational unit vector defined by a polar angle $(0<\theta<\pi)$ and an azimuthal angle $(0<\varphi<2\pi)$. The last term in Eq. (1) is the residual contribution to the free energy due to the repulsive interactions treated at the level of Onsager's second virial theory [1]. The second virial coefficient B_2 is a mole fraction weighted sum of the like B_{11}, B_{22}, and unlike B_{12} terms, so that

$$B_2=x_1^2B_{11}+2x_1x_2B_{12}+x_2^2B_{22}. \tag{2}$$

The other terms in Eq. (1) are the ideal gas term, the ideal entropy of mixing, and a term proportional to the orientational entropy, which is defined in terms of the orientational distribution function of each component as

$$\sigma[f_i]=\int f_i(\boldsymbol{\omega})\ln[4\pi f_i(\boldsymbol{\omega})]d\boldsymbol{\omega}. \tag{3}$$

For hard body fluids, the virial coefficient B_{ij} corresponds to half the orientationally averaged excluded volume between component i and j [43]

$$B_{ij}=\frac{1}{2}\int \nu_{\rm exc}^{ij}(\boldsymbol{\omega}_1,\boldsymbol{\omega}_2)f_i(\boldsymbol{\omega}_1)f_j(\boldsymbol{\omega}_2)d\boldsymbol{\omega}_1 d\boldsymbol{\omega}_2. \qquad (4)$$

The calculation of the excluded volume between two hard spheres of different diameter or between two spherocylinders is reasonably straightforward, and an analytical expression has also been presented for the excluded volume between two cylinders of differing length and diameter [1]. For other nonspherical hard bodies, such as ellipsoids or cut spheres, the calculation of the excluded volume is not straightforward.

In this work we study a binary mixture of rodlike molecules (component 1, characterized by a length L_1 to diameter D_1 ratio L_1/D_1), and platelike molecules (component 2, characterized by a length L_2 to diameter D_2 ratio L_2/D_2) using the theory proposed by Onsager. Onsager's theory is exact in the limit of rodlike particles of infinite aspect ratio, but it quickly becomes inaccurate for less anisotropic molecules; this means that in our study the rodlike molecules are assumed to be very elongated with $L_1 \gg D_1$, while the platelike molecules are assumed to be very flat with $L_2 \ll D_2$ and that $D_2 \gg D_1$. It is important to mention at this stage that while the second virial approach can be justified for fluids of rodlike molecules since the $B_3/B_2^2 \ll 1$, this is not the case for fluids of platelike molecules, and the approximation is more severe in this case [4]. For long and flat molecules, the leading terms of the excluded volumes are given by

$$\nu_{\rm exc}^{11} \sim 2L_1^2 D_1 \sin\gamma,$$

$$\nu_{\rm exc}^{12} \sim \frac{\pi}{4}L_1 D_2^2 |\cos\gamma|, \qquad (5)$$

$$\nu_{\rm exc}^{22} \sim \frac{\pi}{2} D_2^3 \sin\gamma,$$

where $\gamma = \arccos(\boldsymbol{\omega}_i \cdot \boldsymbol{\omega}_j)$ is the angle between particles i and j. It is interesting to note that neither the cross rod-plate, or the plate-plate excluded volumes depend on the thickness of the plate L_2; this is only true at the level of the second virial coefficient, as the free energy is a function of this parameter when the higher virial terms are taken into account.

In order to be consistent with the earlier work of Stroobants and Lekkerkerker [25], we use the virial coefficients of the isotropic phase to characterize the intermolecular parameters,

$$B_{11}^{\rm iso}=\frac{\pi}{4}L_1^2 D_1, \quad B_{12}^{\rm iso}=\frac{\pi}{16}L_1 D_2^2, \quad B_{22}^{\rm iso}=\frac{\pi^2}{16}D_2^3. \qquad (6)$$

These can be obtained by inserting the excluded volumes given by Eq. (5) into Eq. (4), and using the isotropic distribution functions $f_i = 1/(4\pi)$. The molecular parameters are determined by ensuring the virial coefficients are equal for the like rod-rod and plate-plate interactions, and a parameter q is introduced which determines the contribution of the unlike excluded volume in the isotropic phase, so that

$$B_{11}^{\rm iso}=B_{22}^{\rm iso} \quad \text{and} \quad q=\frac{B_{12}^{\rm iso}}{B_{11}^{\rm iso}}. \qquad (7)$$

It is important to note that this relation of the isotropic rod-rod and plate-plate second virial coefficients also means that the like second virial coefficients are equal in the nematic phases. As is customary, a reduced density c is also defined in terms of the rod-rod isotropic virial coefficient as $c = B_{11}^{\rm iso}\rho$. In this way, the mixture is fully defined by the three parameters x, c and q, since a given value of q corresponds to a fixed aspect ratio of the rods (L_1/D_1) and diameters ratio (D_2/D_1) (see Sec. III). Using the new variables, the residual free energy can be written as

$$\rho B_2 = c\frac{4}{\pi}\int [x_1^2 \sin\gamma f_1(\boldsymbol{\omega}_1)f_1(\boldsymbol{\omega}_2)+\pi x_1 x_2 q|\cos\gamma| f_1(\boldsymbol{\omega}_1) \times f_2(\boldsymbol{\omega}_2)+x_2^2\sin\gamma f_2(\boldsymbol{\omega}_1)f_2(\boldsymbol{\omega}_2)]d\boldsymbol{\omega}_1 d\boldsymbol{\omega}_2. \qquad (8)$$

It may be clear at this stage that in order for the free energy [Eq. (1)] to be fully determined, the equilibrium single particle orientational distribution functions $f_i(\boldsymbol{\omega})$ must be known. This can be done by taking the functional derivatives of Eq. (1) while maintaining the normalization conditions $\int f_i(\boldsymbol{\omega})d\boldsymbol{\omega}=1$,

$$\frac{\delta[\beta F/N+\lambda_i(1-\int f_i(\boldsymbol{\omega})d\boldsymbol{\omega})]}{\delta f_i(\boldsymbol{\omega})}=0, \qquad (9)$$

where λ_i are Lagrange undetermined multipliers. The resulting integral equations in our system are

$$\ln[4\pi f_1(\boldsymbol{\omega})]=\lambda_1 - c\left(\frac{8}{\pi}x_1\int \sin\gamma(\boldsymbol{\omega}\cdot\boldsymbol{\omega}_2)f_1(\boldsymbol{\omega}_2)d\boldsymbol{\omega}_2 + 4x_2 q\int |\cos\gamma(\boldsymbol{\omega}\cdot\boldsymbol{\omega}_2)|f_2(\boldsymbol{\omega}_2)d\boldsymbol{\omega}_2\right) \qquad (10)$$

and

$$\ln[4\pi f_2(\boldsymbol{\omega})]=\lambda_2 - c\left(\frac{8}{\pi}x_2\int \sin\gamma(\boldsymbol{\omega}\cdot\boldsymbol{\omega}_2)f_2(\boldsymbol{\omega}_2)d\boldsymbol{\omega}_2 + 4x_1 q\int |\cos\gamma(\boldsymbol{\omega}\cdot\boldsymbol{\omega}_2)|f_1(\boldsymbol{\omega}_2)d\boldsymbol{\omega}_2\right). \qquad (11)$$

The Lagrange multipliers can be eliminated by using the normalization conditions of the orientational distribution functions to give the following integral equations:

$$f_1(\boldsymbol{\omega})=\frac{\exp\left[-c\left(\frac{8}{\pi}x_1\int \sin\gamma(\boldsymbol{\omega}\cdot\boldsymbol{\omega}_2)f_1(\boldsymbol{\omega}_2)d\boldsymbol{\omega}_2+4x_2q\int |\cos\gamma(\boldsymbol{\omega}\cdot\boldsymbol{\omega}_2)|f_2(\boldsymbol{\omega}_2)d\boldsymbol{\omega}_2\right)\right]}{\int \exp\left[-c\left(\frac{8}{\pi}x_1\int \sin\gamma(\boldsymbol{\omega}_1\cdot\boldsymbol{\omega}_2)f_1(\boldsymbol{\omega}_2)d\boldsymbol{\omega}_2+4x_2q\int |\cos\gamma(\boldsymbol{\omega}_1\cdot\boldsymbol{\omega}_2)|f_2(\boldsymbol{\omega}_2)d\boldsymbol{\omega}_2\right)\right]d\boldsymbol{\omega}_1} \tag{12}$$

and

$$f_2(\boldsymbol{\omega})=\frac{\exp\left[-c\left(\frac{8}{\pi}x_2\int \sin\gamma(\boldsymbol{\omega}\cdot\boldsymbol{\omega}_2)f_2(\boldsymbol{\omega}_2)d\boldsymbol{\omega}_2+4x_1q\int |\cos\gamma(\boldsymbol{\omega}\cdot\boldsymbol{\omega}_2)|f_1(\boldsymbol{\omega}_2)d\boldsymbol{\omega}_2\right)\right]}{\int \exp\left[-c\left(\frac{8}{\pi}x_2\int \sin\gamma(\boldsymbol{\omega}_1\cdot\boldsymbol{\omega}_2)f_2(\boldsymbol{\omega}_1)d\boldsymbol{\omega}_1+4x_1q\int |\cos\gamma(\boldsymbol{\omega}_1\cdot\boldsymbol{\omega}_2)|f_1(\boldsymbol{\omega}_1)d\boldsymbol{\omega}_1\right)\right]d\boldsymbol{\omega}_2}. \tag{13}$$

These two equations constitute the starting expressions for the calculation of the phase equilibria in this work, and we discuss different approximations for their solution in the following section. Together with this, the natural thermodynamic function to consider phase stability and equilibria in binary mixtures is the Gibbs free energy (in reduced form $g^*=\beta G/N$), which is derived from the Helmholtz free energy by performing the Laplace transformation

$$g^*=f^*+P^*/c, \tag{14}$$

where the reduced pressure $P^*=\beta PB_{11}^{\mathrm{iso}}$ can be obtained from the reduced Helmholtz free energy $f^*=\beta F/N$ as

$$P^*=c^2\frac{\partial f^*}{\partial c}. \tag{15}$$

By calculating the Gibbs free energy as a function of composition at a given pressure, the phase diagram of the binary mixture can be determined by simply taking the common tangent between the coexisting phases [44]. We follow this method to construct the phase diagram of the present system.

A. L2 solution

1. Isotropic-nematic bifurcation

The coupled integral equations (12) and (13) are quite difficult to solve analytically, but they simplify substantially by expanding the kernels of the integrals in terms of Legendre polynomials. In the so-called L2 approximation the expansion is truncated at second order, so that

$$\sin\gamma\approx\frac{\pi}{4}-\frac{5\pi}{32}P_2(\cos\gamma),$$

$$|\cos\gamma|\approx\frac{1}{2}+\frac{5}{8}P_2(\cos\gamma). \tag{16}$$

If we define the uniaxial order parameters as the orientational averages of the second Legendre polynomials

$$S_i=\int P_2(\cos\theta)f_i(\boldsymbol{\omega})d\boldsymbol{\omega}, \tag{17}$$

the orientational distribution functions [Eqs. (12) and (13)] can be expressed as functions of the uniaxial order parameters of the two components, given now by

$$f_1(\theta)=\frac{\exp[\frac{5}{4}c(x_1S_1-2x_2qS_2)P_2(\cos\theta)]}{\int \exp[\frac{5}{4}c(x_1S_1-2x_2S_2)P_2(\cos\theta_1)]d\boldsymbol{\omega}_1} \tag{18}$$

and

$$f_2(\theta)=\frac{\exp[\frac{5}{4}c(x_2S_2-2x_1qS_1)P_2(\cos\theta)]}{\int \exp[\frac{5}{4}c(x_2S_2-2x_1qS_1)P_2(\cos\theta_1)]d\boldsymbol{\omega}_1}. \tag{19}$$

In the derivation of these equations we have assumed that the orientational ordering is symmetrical around the nematic director taken in the direction of z axis (as expected for a uniaxial phase). Moreover, we have used the L2 approximation [Eq. (16)] and the addition theorem of spherical harmonics [45], such that

$$P_2(\cos\gamma)=P_2(\cos\theta_1)P_2(\cos\theta_2)+2\sum_{i=1}^{2}\frac{(2-i)!}{(2+i)!}\times P_2^i(\cos\theta_1)P_2^i(\cos\theta_2)\cos[i(\varphi_1-\varphi_2)]. \tag{20}$$

It is important to note that the terms proportional to the associated Legendre polynomials (P_n^i) will vanish in this case since the nematic phase is uniaxial and does not depend on the azimuthal angle. In the following section, where the biaxial nematic phase is considered, one of the terms of the two associated Legendre polynomials (P_2^2) has a finite contribution. Equations (18) and (19) were derived by Stoobants and Lekkerkerker [25] in the context of mixtures of rodlike and platelike particles; earlier, Flapper and Vertogen [46] had also used the L2 approximation in a pure rod system.

After multiplying by the second Legendre polynomials on both sides of Eqs. (18) and (19), and integrating both sides, a set of self-consistent equations can be obtained for the order parameters in the mixture, which can then be solved numerically [47]. However, an important insight can also be gained from Eqs. (18) and (19) when a weakly ordered nematic phase is considered. When S_1 and $S_2 \to 0$ the exponentials in Eqs. (18) and (19) can be expanded using the familiar Taylor series up to second order ($\exp x \approx 1+x$) giving

$$f_1(\theta) = \frac{1 + \frac{5}{4}(x_1 S_1 - 2q x_2 S_2) c P_2(\cos\theta)}{4\pi} \tag{21}$$

and

$$f_2(\theta) = \frac{1 + \frac{5}{4}(x_2 S_2 - 2q x_1 S_1) c P_2(\cos\theta)}{4\pi}. \tag{22}$$

The corresponding equations for the order parameters are

$$S_1 = x_1 c S_1/4 - q x_2 c S_2/2 \tag{23}$$

and

$$S_2 = x_2 c S_2/4 - q x_1 c S_1/2. \tag{24}$$

The elimination of the order parameters results in a quadratic equation for the reduced density c,

$$0 = (1 - 4q^2) x_1 x_2 c^2 - 4c + 16. \tag{25}$$

In this way, it is possible to determine the density at which the nematic phase bifurcates from the isotropic phase without solving the coupled integral equations. However, it must be noted that this equation gives only an upper limit for the isotropic phase stability without determining the nature of the isotropic-nematic phase transition; the isotropic-nematic phase transition may take place at lower densities than indicated by Eq. (25). The incorporation of an additional term in the Taylor expansion of the exponentials results in slightly more complex coupled equations for the order parameters; in this case, the density dependence of the order parameters including the bifurcation point is obtained, together with the correct order of the phase transition. Unfortunately, this expansion underestimates the order parameters for dense nematic phases and so we do not present these equations here [48]. Equations (23) and (24) also provide the order parameters of the two components in such a way that they are interdependent. It can be seen from the expressions that if the order parameter of one component is positive (determining the nematic director), the order parameter of the second component must be negative; this means that the symmetry axes of the two components align in perpendicular directions with respect to each other. One should also note, however, that the second component is randomly oriented within the perpendicular plane (so-called planar phase). A large average excluded volume is associated with such planar ordering, and as a consequence, the possibility of biaxial order (additional ordering in the plane perpendicular to the uniaxial director) cannot be excluded in this system, as this will increase the free volume (translational) entropy.

2. Nematic-biaxial nematic bifurcation

In a rod-rich uniaxial nematic phase, the rods pack very effectively, maximizing the packing entropy, but the plates in this planar configuration do not significantly increase the free-volume entropy with respect to the isotropic phase. The free-volume entropy is increased by additional ordering in the direction perpendicular to the alignment of rods (biaxial ordering); this gives rise to azimuthal anisotropy in the orientational distribution functions.

In considering the possibility of biaxial ordering, Eqs. (18) and (19) have to be expressed in a more general form; in the case of the L2 approximation [Eq. (16)] together with Eq. (20) the corresponding expressions are

$$f_1(\theta,\varphi) = \frac{\exp[\frac{5}{4}c(x_1 S_1 - 2x_2 q S_2) P_2(\cos\theta) + \frac{5}{4}c(x_1 \Delta_1 - 2x_2 q \Delta_2) D(\theta,\varphi)]}{\int \exp[\frac{5}{4}c(x_1 S_1 - 2x_2 q S_2) P_2(\cos\theta_1) + \frac{5}{4}c(x_1 \Delta_1 - 2x_2 q \Delta_2) D(\theta_1,\varphi_1)] d\boldsymbol{\omega}_1} \tag{26}$$

and

$$f_2(\theta,\varphi) = \frac{\exp[\frac{5}{4}c(x_2 S_2 - 2x_1 q S_1) P_2(\cos\theta) + \frac{5}{4}c(x_2 \Delta_2 - 2x_1 q \Delta_1) D(\theta,\varphi)]}{\int \exp[\frac{5}{4}c(x_2 S_2 - 2x_1 q S_1) P_2(\cos\theta_1) + \frac{5}{4}c(x_2 \Delta_2 - 2x_1 q \Delta_1) D(\theta_1,\varphi_1)] d\boldsymbol{\omega}_1}, \tag{27}$$

where the biaxial order parameters

$$\Delta_i = \int f_i(\theta,\varphi) D(\theta,\varphi) d\boldsymbol{\omega}, \tag{28}$$

have been introduced using a function $D(\theta,\varphi)$ defined from the second associated Legendre polynomial P_2^2,

$$D(\theta,\varphi) = \frac{\sqrt{3}}{2} \sin^2\theta \cos(2\varphi).$$

As before, it is possible to expand the exponential functions in Eqs. (26) and (27) in the vicinity of the nematic–biaxial nematic bifurcation point, i.e., $\Delta_1 \to 0$ and $\Delta_2 \to 0$. It can be seen that the orientational distribution functions bifurcate from the uniaxial nematic distributions $f_{i,N}$ with the $D(\theta,\varphi)$ function, since

$$f_1(\theta,\varphi)=f_{1,N}(\theta)[1+\tfrac{5}{4}(x_1\Delta_1-2qx_2\Delta_2)cD(\theta,\varphi)] \tag{29}$$

and

$$f_2(\theta,\varphi)=f_{2,N}(\theta)[1+\tfrac{5}{4}(x_2\Delta_2-2qx_1\Delta_1)cD(\theta,\varphi)]. \tag{30}$$

Integrating both sides of Eqs. (29) and (30) with $D(\theta,\varphi)$, and using the orthogonal property of this function, expressions for the biaxial order parameters are obtained for each of the components,

$$\Delta_1=\frac{5}{4}c\left(x_1\Delta_1\int D^2(\theta,\varphi)f_{1,N}(\theta)d\boldsymbol{\omega}\right.$$
$$\left.-2qx_2\Delta_2\int D^2(\theta,\varphi)f_{1,N}(\theta)d\boldsymbol{\omega}\right) \tag{31}$$

and

$$\Delta_2=\frac{5}{4}c\left(x_2\Delta_2\int D^2(\theta,\varphi)f_{2,N}(\theta)d\boldsymbol{\omega}\right.$$
$$\left.-2qx_1\Delta_1\int D^2(\theta,\varphi)f_{2,N}(\theta)d\boldsymbol{\omega}\right). \tag{32}$$

On eliminating the biaxial order parameters the bifurcation equation for the L2 approximation is obtained as

$$25c^2(1-4q^2)x_1x_2\int D^2f_{1,N}d\boldsymbol{\omega}\int D^2f_{2,N}d\boldsymbol{\omega}$$
$$-20c\left(x_1\int D^2f_{1,N}d\boldsymbol{\omega}+x_2\int D^2f_{2,N}d\boldsymbol{\omega}\right)+16=0. \tag{33}$$

The nematic–biaxial nematic bifurcation density is determined from this equation by using the uniaxial orientational distribution functions given in Eqs. (18) and (19). An interesting feature of Eq. (33) is that it reduces to the isotropic-nematic bifurcation [Eq. (25)] if the orientational distribution functions are isotropic, meaning that there is no direct isotropic–biaxial nematic transition in the L2 approximation. This will become apparent in the discussion of our results.

B. Numerical solution

The use of simple approximations to obtain the equilibrium orientational distribution functions in ordered phases, such as trial function methods [43] or the L2 model [25,41] discussed earlier have the obvious advantage of relative mathematical simplicity. It is clear that in each case these approximations introduce some degree of error. For example, it has already been pointed out in previous work [18] that these approximations may result in a qualitatively incorrect conclusion about the existence of a critical point in nematic-nematic phase boundaries of rod-rod binary mixtures.

In the present model the accurate solution of the Euler-Lagrange equations is even more important, because of the subtle competition between the entropy of mixing and the unlike excluded volume which determines the stability of the biaxial nematic phase. The shortcomings of the series expansion methods can be demonstrated by calculating the absolute difference between an orientationally dependent function $\Gamma(\gamma)$ and its Legendre polynomial representation

$$\chi_n(\gamma)=\left|\Gamma(y)-\sum_{i=0}^{n}a_iP_i(\cos\gamma)\right|, \tag{34}$$

where a_i is the corresponding coefficient of the Legendre expansion of the function. We have evaluated the function for the integral kernels [i.e., $\sin\gamma$ and $|\cos\gamma|$] up to 18th order [note that Eq. (16) presents the expansion only up to second order], and the results are depicted in Fig. 1. It is clear from the figure that the expansion converges very slowly, and that the error is particularly large for the parallel and perpendicular directions. Hence, it is rather questionable whether the second-order approximation (L2 model) or even high-order expansions are adequate for a reliable quantitative (and even qualitative) description of the phase equilibria.

In order to test the accuracy and reliability of the L2 solution presented in the preceding section we solve the coupled integral equations (12) and (13) entirely numerically (i.e., without approximations). The integration over the orientational unit vector ($\boldsymbol{\omega}$) is carried out by Simpson's quadrature. We ensure that the polar (θ) and azimuthal (φ) parts of $\boldsymbol{\omega}$ are treated at the same level by considering an interval $[0,\pi]$ for θ and an interval $[0,2\pi]$ for φ, and both are divided into subintervals of the same grid size. In order to maximize the accuracy of the numerical approach, while minimizing the computational burden, the optimal grid size is determined by solving integral equations (12) and (13) in the uniaxial nematic phase, where the calculation of the orientational distribution function depends only on the polar angle (θ). We find that the minimum number of intervals between $[0,\pi]$ must be at least 40. Using the grid size obtained for the uniaxial nematic phase, Eqs. (12) and (13) are solved iteratively: guesses are made for $f_1(\boldsymbol{\omega})$ and $f_2(\boldsymbol{\omega})$, which are substituted into the right-hand side of the equations to obtain a new pair of $f_1(\boldsymbol{\omega})$ and $f_2(\boldsymbol{\omega})$; in each iterative step the new solution is mixed with the previous one so that the old function is 90% of the new one (this ensures the convergence of the method) and the procedure is repeated until the $\max|f_{i,\mathrm{new}}(\boldsymbol{\omega})-f_{i,\mathrm{old}}(\boldsymbol{\omega})|<10^{-9}$ $(i=1,2)$. The director defining the nematic phase is not unique in these systems. In the case of a uniaxial nematic phase the integration over the second azimuthal angle means that the director lies along the z axis in order to be consistent with uniaxial ordering. In the case of a biaxial nematic phase this is no longer possible because the solution also depends on the azimuthal angles. In order to fix the main nematic director along the z axis (as before), a biaxial initial guess of the orientational distribution function is made such that the director is oriented along this axis; this is equivalent to the pinning of the main nematic director. Finally, the coexistence

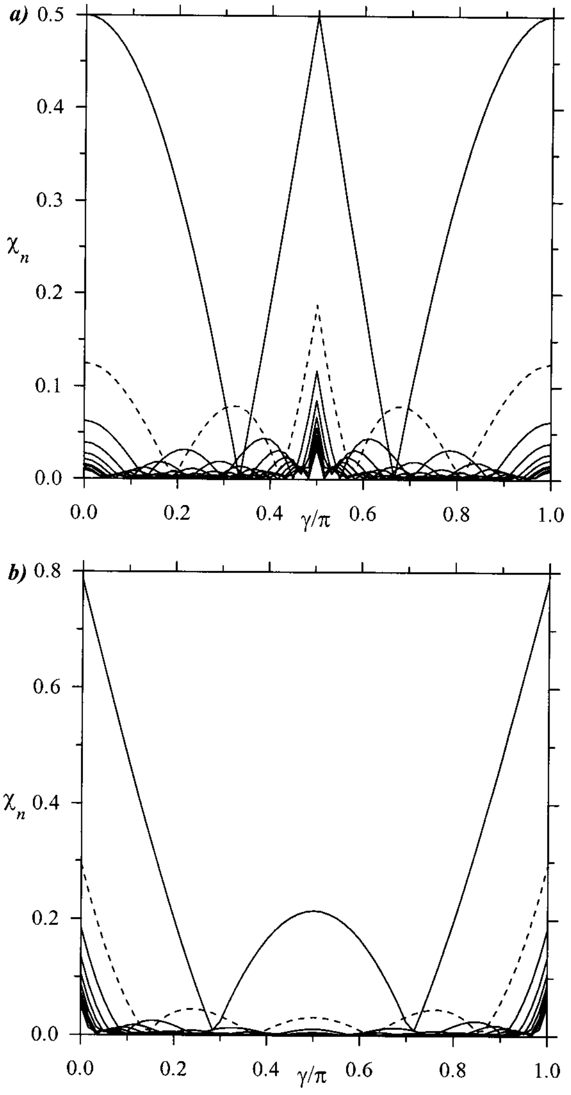

FIG. 1. Error of the Legendre polynomial expansion method for (a) $|\cos\gamma|$ and (b) $(\sin\gamma)$ as a function of the angle γ. The error is calculated as indicated in Eq. (34). The values of n presented are (from top to bottom in both parts): 0, 2 (dashed curve), 4, 6, 8, 10, 12, 14, 16, and 18.

conditions (equality of pressure and chemical potentials) involving phases of different symmetry are solved using the downhill simplex method [47]; the accuracy in the coexistence pressure $P=-\partial F/\partial V$ and chemical potentials $\mu_i=\partial F/\partial N_i$ is chosen to be of at least six significant figures.

C. Demixing transitions

In addition to the isotropic-nematic and nematic-biaxial phase transitions which have already been discussed, a mixture of rodlike and platelike hard particles of differing size may exhibit demixing in phases of the same symmetry (i.e., isotropic-isotropic or nematic-nematic demixing). In the case of our mixture of purely repulsive particles there is no vapor-liquid phase transition. A given phase is stable if the second derivative of the Gibbs free energy with respect to the mole fraction is positive, which in our reduced units is expressed as

$$\left(\frac{\partial^2 g^*}{\partial x^2}\right)_P>0, \tag{35}$$

where we use the notation x for the mole fraction of one of the components. Written as a function of the reduced free energy $f^*=\beta F/N$, the second derivative of the Gibbs free energy is given by

$$\left(\frac{\partial^2 g^*}{\partial x^2}\right)_P=\left(\frac{\partial^2 f^*}{\partial x^2}\right)_c-c\,\frac{\left(\dfrac{\partial^2 f^*}{\partial x\,\partial c}\right)^2}{\left(2\,\dfrac{\partial f^*}{\partial c}+c\,\dfrac{\partial^2 f^*}{\partial c^2}\right)_x}, \tag{36}$$

where we have taken advantage of the fact that f^* depends only on x and c, and have used the Euler chain relations. The spinodal boundary (demixing limit) is obtained when this expression is equal to zero [44], so that substituting Eq. (1) into Eq. (36) gives the general equation for the spinodal curve of the phases studied in this work,

$$\begin{aligned}1&+c\,\frac{8}{\pi}x\int(x_1f_1f_1+x_2f_2f_2)\sin\gamma\, d\boldsymbol{\omega}_1 d\boldsymbol{\omega}_2\\&-4c^2x_1x_2\Bigg[q^2 4\left(\int|\cos\gamma|f_1f_2\,d\boldsymbol{\omega}_1 d\boldsymbol{\omega}_2\right)^2\\&-\frac{16}{\pi^2}\int f_1f_1\sin\gamma\, d\boldsymbol{\omega}_1 d\boldsymbol{\omega}_2\int f_2f_2\sin\gamma\, d\boldsymbol{\omega}_1 d\boldsymbol{\omega}_2\Bigg]=0.\end{aligned} \tag{37}$$

In particular, the isotropic-isotropic demixing spinodal line is obtained from Eq. (37) by inserting the isotropic distribution functions $f_i=1/(4\pi)$, which gives a simple quadratic equation

$$1+2c-4x_1x_2(q^2-1)c^2=0. \tag{38}$$

The boundary can be seen to be symmetrical in composition (about $x=1/2$). The determination of the demixing spinodal curve is very useful in such mixtures, as it provides the boundary of phase separation without requiring an explicit solution of the phase coexistence. In the particular case involving symmetric mixtures, the compositions of the rod-rich and plate-rich coexisting phases coincide with the minima of the Gibbs function in demixing transitions involving phases of the same symmetry (i.e., isotropic-isotropic and nematic-nematic transitions); this is due to the fact that the Gibbs surface is symmetric with respect to $x=0.5$ since the rod-rod and plate-plate excluded volumes are equal. Hence, in terms of derivatives of the reduced Gibbs function, a relation

$$\left(\frac{\partial g^*}{\partial x}\right)_p=0 \tag{39}$$

can be used to determine the phase equilibria in the special cases mentioned above. This relation can be rewritten in a more convenient way as a function of the reduced Helmholtz free energy as

$$\left(\frac{\partial g^*}{\partial x}\right)_p=\left(\frac{\partial f^*}{\partial x}\right)_c. \tag{40}$$

In this way, the solution of the phase coexistence conditions is avoided by simply taking the derivative of f^* with respect to the mole fraction, so that using Eq. (40) a relatively simple equation for the demixing phase boundary of the rod-plate mixture is given by

$$\begin{aligned}\ln\left(\frac{x_2}{x_1}\right)+\sigma[f_2]-\sigma[f_1]+4c\bigg\{\int\bigg(&\frac{2}{\pi}x_2\sin\gamma f_2f_2+(x_1-x_2)\\ &\times q|\cos\gamma|f_1f_2-\frac{2}{\pi}x_1\sin\gamma f_1f_1\bigg)d\boldsymbol{\omega}_1d\boldsymbol{\omega}_2\bigg\}\\ =0. \end{aligned} \tag{41}$$

It is important to note that this equation cannot be solved analytically for the uniaxial or the biaxial nematic phases, because of the density dependence of the orientational distribution functions. In these cases we use the numerical Newton-Raphson method [47]. For the isotropic phase, the solution is much simpler, and the reduced density can be expressed as a function of q and x as

$$c_{\text{I-I}}=\frac{\ln\left(\frac{x_1}{x_2}\right)}{2[x_2-x_1-(x_2-x_1)q]}, \tag{42}$$

which is again found to be symmetrical about composition. If $x_1=x_2=1/2$ this equation is even simpler giving,

$$c_{\text{I-I}}=\frac{1}{(q-1)}. \tag{43}$$

This clearly indicates that isotropic-isotropic (I-I) demixing does not take place for $q<1$, but that it is possible for isotropic-isotropic demixing to occur in mixtures with $q>1$. Of course, this does not mean that the system will demix into a rod-rich and a plate-rich isotropic phase for all $q>1$, as a favorable ordering into a nematic phase may preempt this transition. The delicate balance between the orientational free volume and mixing entropies gives rise to a wealth of phase behavior as will become clear in the following section.

III. RESULTS

We study the phase behavior for our symmetric mixture of rod and plate molecules taking into account isotropic, nematic, and biaxial nematic phases. We carry out a bifurcation analysis, and determine the phase coexistence boundaries using the second virial theory of Onsager; two approaches are used to solve kernels of the integrals, an expansion in Legendre polynomials up to second order (L2 approximation), and a numerical solution that involves no approximations. We investigate the global phase behavior of the mixture in terms of the molecular parameters, studying the effect of different rod-plate unlike excluded volume contributions, characterized by the parameter q [Eq. (7)]. A change of the unlike excluded volume does not of course give rise to a different phase behavior of the pure components, even though this would correspond to different molecular aspect ratios in each case and to different transition densities; this is a direct result of the theory of Onsager, in which the concentration has been written in terms of the rod dimensions. It should be noted that, due to the fact that the approach of Onsager is a second virial theory, it is accurate only in the case of very long and thin rods, and care needs to be taken not to change the value of the unlike excluded volume q in a way that the aspect ratio of the rods becomes too small making the theory inaccurate. In this work we present the phase behavior of rod-plate mixtures for values of q ranging from 0.5 to 1.6.

The aspect ratio ($\kappa=L_1/D_1$) and the diameter ratio ($\kappa'=D_2/D_1$) are determined from the value of q through the following relations: $\kappa=4\pi^2q^3$ and $\kappa'=4\pi q^2$. Throughout this section, we report the aspect and diameter ratios for corresponding values of the q parameter and denote the mole fraction of the plates as x. The results obtained using the L2 approximation are presented before those of the full numerical solution.

A. Phase behavior in the L2 approximation

The L2 approximation of the excluded volume is rather crude as we have seen in the comparisons shown in Fig. 1. The advantage of the L2 approach is, however, that it is possible to get an indication of the phase behavior of the mixture without the need for a full solution. Instead of solving the system of integral equations given by Eqs. (18) and (19), we start by examining the isotropic-nematic bifurcation [Eq. (25)] and the isotropic-isotropic spinodal [Eq. (38)] boundaries. Equation (25) is quadratic in the reduced density c and can easily be solved, giving the known pure fluid bifurcation limit of $c=4$ [49]; it is clearly symmetric in mole fraction (the same bifurcation density is found for both pure components since their second virial coefficients are the same $B_{11}=B_{22}$). It is interesting to note that when the unlike excluded volume parameter is $q=0.5$ the isotropic-nematic bifurcation density is independent of the mole fraction with a constant value of $c=4$, while for lower or higher q, the bifurcation densities of the mixture increase or decrease, respectively (see Fig. 2). The bifurcation curves give an indication of the relative stability of nematic and isotropic phases with respect to each other, suggesting that for our model with $q<0.5$ a destabilization of the nematic phase with respect to the isotropic phase is predicted. In contrast with this, the conclusions of previous theoretical [25,41] and simulation studies [38,39] suggest that there is a tendency to stabilize the nematic phase on mixing. A more recent Monte Carlo simulation study of a near-symmetric binary mixture of hard spherocylinders and hard cut spheres indicates that there is a destabilization of the nematic phase in such mixtures [40].

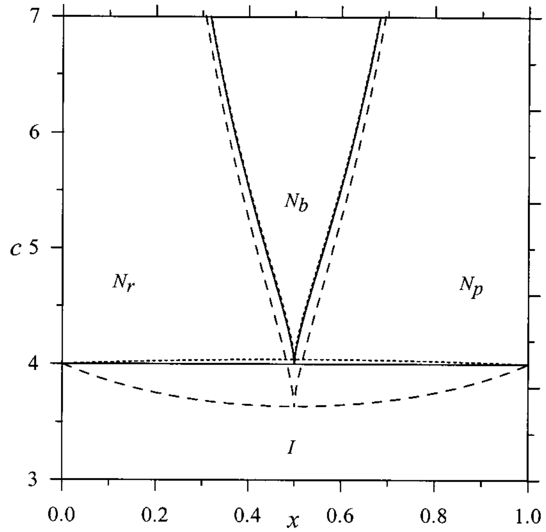

FIG. 2. Bifurcation phase diagram of the symmetric mixture of rods and plates for $q=0.49$ (short dashed curves), 0.5 (continuous curves), and 0.6 (long dashed curves) in the reduced density-composition plane. The labels I, N_r, N_p, and N_b denote isotropic, rod-rich nematic, plate-rich nematic, and biaxial nematic phases, respectively. x corresponds to the mole fraction of the plates.

The rod aspect ratio and plate-rod diameter ratio of the model simulated in Ref. [40] ($\kappa=5$, $\kappa'=3.62$) are very close to those corresponding to $q=0.5$ ($\kappa=4.93$ and $\kappa'=3.14$) in our present work. It is not useful, however, to attempt a quantitative comparison of the theoretical results presented in our current work with the simulation data [40] as the aspect ratios involved are too small for the Onsager theory to be accurate. Furthermore, the simulations were carried out for a mixture of hard spherocylinders and hard cut-spheres, while in our theoretical model the particles are cylindrical in shape as the end effects in the excluded volume have been neglected. It should also be noted that the liquid-crystalline phase obtained for the cut-sphere fluid in the simulation exhibits columnar positional order instead of just nematic orientational order. Having acknowledged the important point that our theoretical predictions for the small values of q yield quantitatively inaccurate results, we use the low q results as a starting point in our examination of the phase behavior for larger values of q where the Onsager theory is known to be much more accurate.

The nematic-biaxial nematic bifurcation line can be located using Eq. (33) together with the orientational distribution functions given in Eqs. (18) and (19), which are obtained by iteration. It can be seen from the bifurcation expression that an increase in the unlike interaction q promotes the biaxial nematic phase; a larger value of the parameter q extends the stability of the biaxial phase to lower densities (and lower pressures) and to wider ranges of composition (see Fig. 2). It is also apparent that the isotropic-nematic and nematic–biaxial nematic bifurcation boundaries always meet at an equimolar composition, which suggests that the isotropic-nematic transition is second order at this point, as the bifurcation equations (25) and (33) are identical for isotropic distributions of the particles.

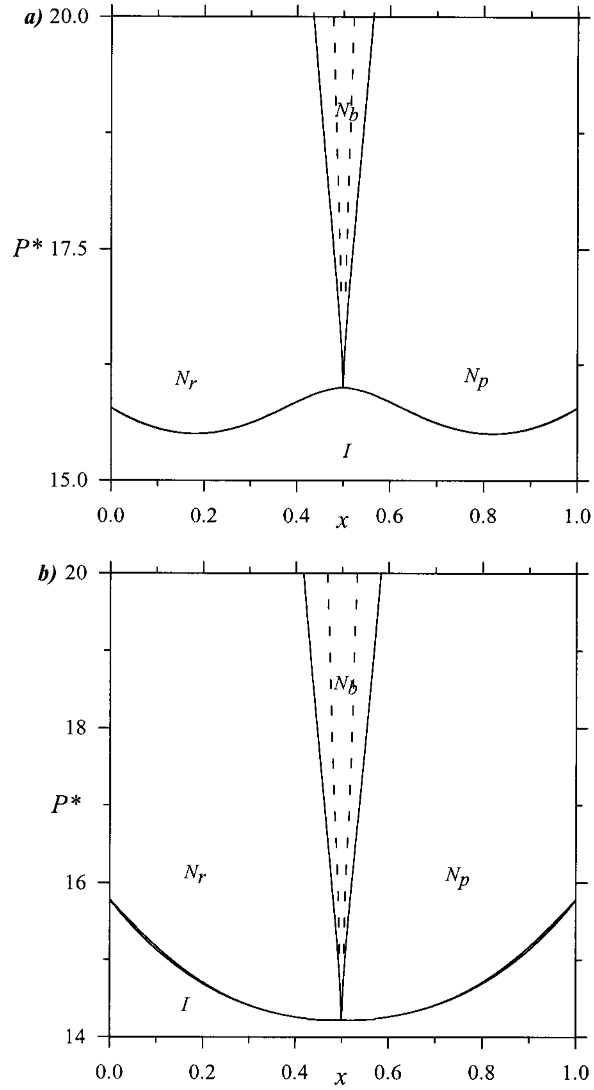

FIG. 3. Pressure-composition (P^*x) representation of the phase diagram for a symmetric mixture of rods and plates obtained with the L2 approximation for (a) $q=0.5$ and (b) $q=0.6$. The continuous curves represent the stable coexistence curves of the isotropic-nematic and nematic–biaxial nematic transitions, while the dashed curves indicate the metastable nematic-nematic demixing transition. The labels I, N_r, N_p, and N_b denote isotropic, rod-rich nematic, plate-rich nematic, and biaxial nematic phases, respectively. x corresponds to the mole fraction of the plates.

The full phase diagrams of the rod-plate binary mixture have been calculated for $q=0.5$ to 1.6. As has already been mentioned, the theory of Onsager at the level of the second virial coefficient becomes very inaccurate for smaller aspect ratios. It significantly overestimates the transition densities (a value of $q=0.63$ corresponds to rods with an aspect ratio of about 10, for which the Onsager approach starts providing a more quantitative description [43]). Furthermore, the approach does not take into account the positionally ordered phases such as smectic A and columnar phases that are favored for smaller aspect ratios. In Fig. 3(a) the pressure-composition phase diagram obtained with the L2 approximation for a mixture with $q=0.5$ (corresponding to a rod aspect ratio of $\kappa=4.93$ and a plate-rod diameter ratio of $\kappa'=3.14$) is shown. The isotropic-nematic bifurcation curve was found to be independent of composition for $q=0.5$ (see Fig. 2). When the coexistence boundaries are examined for this system one finds that for the rod-rich ($x\lesssim 0.2$) or plate-rich ($x\gtrsim 0.8$) phases mixing destabilizes the isotropic phase relative to the nematic phase (favoring ordering), while for mixtures close to the equimolar composition ($x=0.5$) the ordered phase is destabilized. As a result, two isotropic-nematic azeotropes at about $x=0.2$ and 0.8 are observed in the phase diagram. The isotropic-nematic phase transition is found to be weakly first order (except at $x=0.5$ where the transition is continuous) so that the boundaries depicted in Fig. 3(a) actually correspond to two curves, one for the isotropic compositions and the other for the nematic compositions. In the case of the systems with large q these two phase regions will become clearly visible [cf. Fig. 3(b)]. In the high-pressure region, two nematic phases are observed (one rich in rods and one rich in plates), together with a stable biaxial nematic phase for intermediate compositions, the extent of the biaxial nematic phase is seen to decrease with decreasing pressure (as suggested by the bifurcation study). The nematic-biaxial nematic transition is found to be second order. At $x=0.5$, four phases (isotropic, rod-rich nematic, plate-rich nematic, and biaxial phase) merge into one at a multicritical point. This point also corresponds to the lowest pressure at which the biaxial nematic phase is observed.

The phase diagram obtained with the L2 approximation for a mixture with $q=0.6$ ($\kappa=8.5$ and $\kappa'=4.5$) presented in Fig. 3(b) is very similar to that obtained by Stroobants and Lekkerkerker [25] for $q=1$. The only difference is that the isotropic-nematic coexistence, as well as the biaxial nematic region are found to be less extensive for $q=0.6$.

As was mentioned earlier, it is also important to check the stability of the biaxial nematic phase with respect to nematic-nematic phase separation [using Eq. (41) and computing the Gibbs free energy]. For values of the unlike excluded volume parameter of $q=0.5$ and $q=0.6$ the nematic-nematic demixing transition is always metastable for all of the pressures studied [the dashed curves shown Figs. 3(a) and 3(b) denote the demixing boundaries]. At higher pressures, the system may demix into a rod-rich and a plate-rich nematic phase (or even into two more ordered smectic *A* and columnar phases) due to the increasing importance of excluded volume effects. Indeed, nematic-nematic demixing is found to be stable at pressures above the biaxial nematic phase for a mixture with $q=1.4$ (corresponding to large aspect and diameter ratios of $\kappa=108.3$ and $\kappa'=24.6$) as can be seen in Fig. 4.

The bifurcation curves for the isotropic-nematic transition [Eq. (25)] together with the isotropic-isotropic demixing spinodal curves [Eq. (38)] are shown in Fig. 5 for mixtures with $q=1.5$ and $q=1.6$. In the preceding section we pointed out that isotropic-isotropic demixing is not stable for $q<1$, and that a competition between the isotropic-isotropic demixing spinodal line and the isotropic-nematic bifurcation line determines the stability of the phase transition. Since both equations are symmetric in the mole fraction, it is evident that the two lines will first meet at the equimolar composition. By simultaneously solving the quadratic expressions given in Eqs. (25) and (38) at $x=0.5$, it can be shown that the bifurcation curves will meet when $q=1.5$ and $c=2$ [see Figs. 5 and 6(a)]. For values of $q>1.5$ (see Fig. 5) the spinodal demixing of the isotropic phase occurs at lower pressures (and densities) than the isotropic-nematic bifurcation for certain ranges of composition.

An examination of the phase diagram of the mixture with $q=1.5$ ($\kappa=133.2$ and $\kappa'=28.3$) [see Fig. 6(a)] indicates that

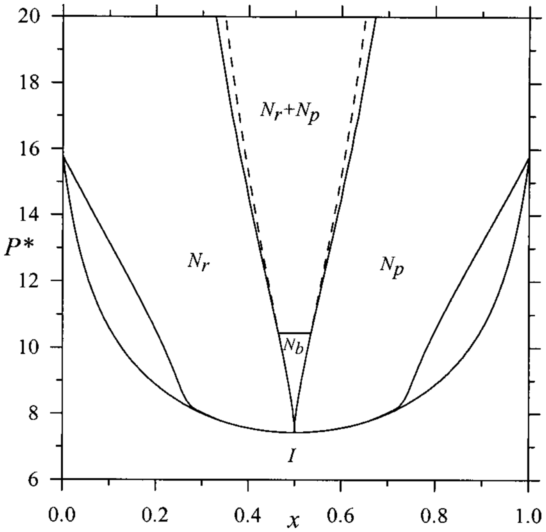

FIG. 4. Pressure-composition (P^*x) representation of the phase diagram for a symmetric mixture of rods and plates obtained with the L2 approximation for $q=1.4$. The continuous curves correspond to the stable transitions, and the dashed curves to the metastable nematic−biaxial nematic phase boundary. The labels *I*, N_r, N_p, and N_b denote isotropic, rod-rich nematic, plate-rich nematic, and biaxial nematic phases, respectively. *x* corresponds to the mole fraction of the plates.

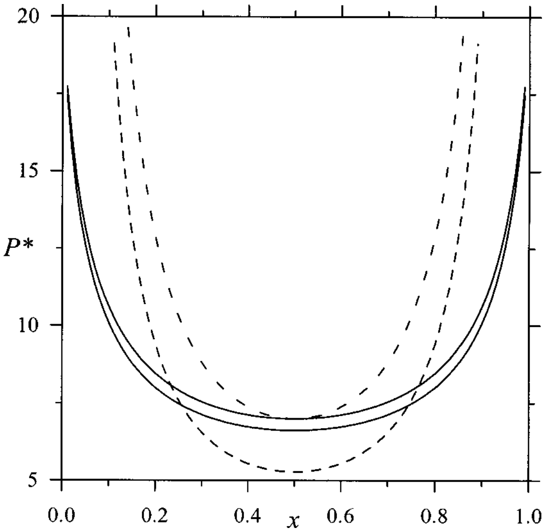

FIG. 5. Stability of the isotropic-nematic bifurcation (continuous curves) with respect to the isotropic-isotropic spinodal decomposition (dashed curves) for $q=1.5$ and 1.6. The curves meeting at the equimolar composition correspond to a mixture with $q=1.5$, while the other two curves correspond to $q=1.6$.

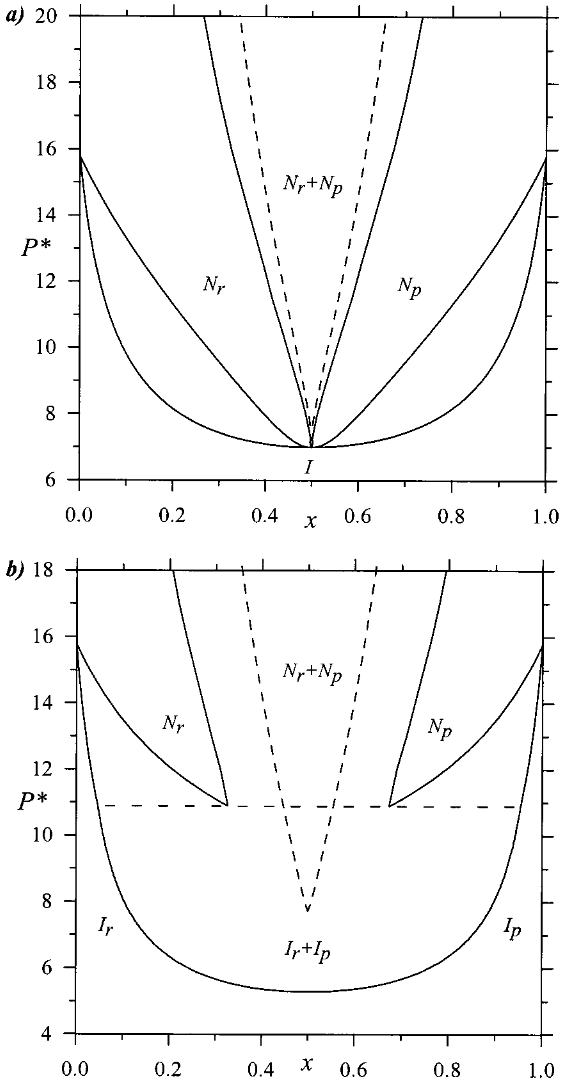

FIG. 6. Pressure-composition (P^*x) representation of the phase diagram for a symmetric mixture of rods and plates obtained with the L2 approximation for (a) $q=1.5$ and (b) $q=1.6$. The continuous curves represent the stable coexistence curves of the isotropic-nematic and nematic-nematic transitions, while the dashed curves indicate the metastable nematic-biaxial nematic transition. The additional labels I_r and I_p denote a rod-rich isotropic phase and a plate-rich isotropic phase, respectively.

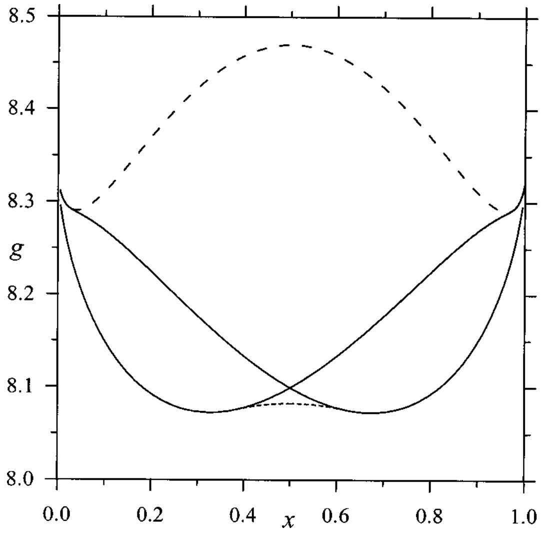

FIG. 7. Gibbs free energy density versus composition for a symmetric mixture of rods and plates obtained with the L2 approximation for $q=1.5$ and $P^*=16$. The continuous curves indicate the stable rod-rich and plate-rich nematic solutions, while the long- and short-dashed curves are the metastable isotropic and biaxial nematic solutions, respectively.

the biaxial phase is entirely preempted by demixing into two nematic phases, but no demixing of the isotropic phase is seen. A stable isotropic-isotropic demixing region can be seen in Fig. 6(b), which corresponds to a mixture with $q=1.6$ ($\kappa=161.7$ and $\kappa'=32.2$). The isotropic-isotropic demixing curve is calculated using Eq. (42) while the nematic-nematic demixing curve is obtained from Eq. (41). At high pressure nematic-nematic demixing is observed in this mixture, while in the intermediate pressure range isotropic-isotropic demixing is seen. The magnitude of this immiscibility is quite remarkable, it is very extensive in composition and pressure, and ends at a critical pressure minimum at which the two isotropic phases merge. The nematic-nematic coexistence region meets the isotropic-isotropic region at a four-phase coexistence line close to $P^*=11$.

Before we conclude our discussion of the results obtained with the L2 approximation it is also useful to consider the Gibbs free energy of each of the phases studied for the mixture with $q=1.5$. It can be seen in Fig. 7 that at a reduced pressure of $P^*=16$, the Gibbs free energy of the biaxial nematic phase is always higher than the Gibbs free energy of the coexisting nematic rod-rich and plate-rich phases. The isotropic free energy curve would correspond to a demixed phase, but it is clearly metastable with respect to the nematic phases.

B. Phase behavior using the numerical solution

At this stage it is useful to note that the L2 approximation overpredicts the isotropic-nematic transition pressures of the pure components; in the L2 approximation the reduced pressure of the isotropic-nematic transition is $P^*_{\text{I-N}}=15.79$, while a pressure $P^*_{\text{I-N}}=14.12$ is obtained when the full numerical solution is used [49]. However, in the case when $q=0.5$, the equimolar isotropic-nematic bifurcation pressure is $P^*=16$ for both solutions, so that it is clear that the isotropic phase must be stabilized and orientational ordering is less favorable close to $x=0.5$ both in the L2 model and with the numerical procedure. The large difference in pressure at $x=0$ and $x=0.5$ suggests that the stabilization of the isotropic phase must start close to the pure component axes ($x\rightarrow 0$ and $x\rightarrow 1$). In order to resolve this question, we investigate the phase diagrams of the rod-plate mixture for $q=0.5$ and $q=0.6$ [Figs. 8(a) and 8(b)] with the numerical solution. In the case when $q=0.5$ the isotropic phase is seen to become more stable for most of the composition range; close to $x=0$ and $x=1$ a slight minimum in pressure is observed. Compared to the L2 calculations with the same value of q, both

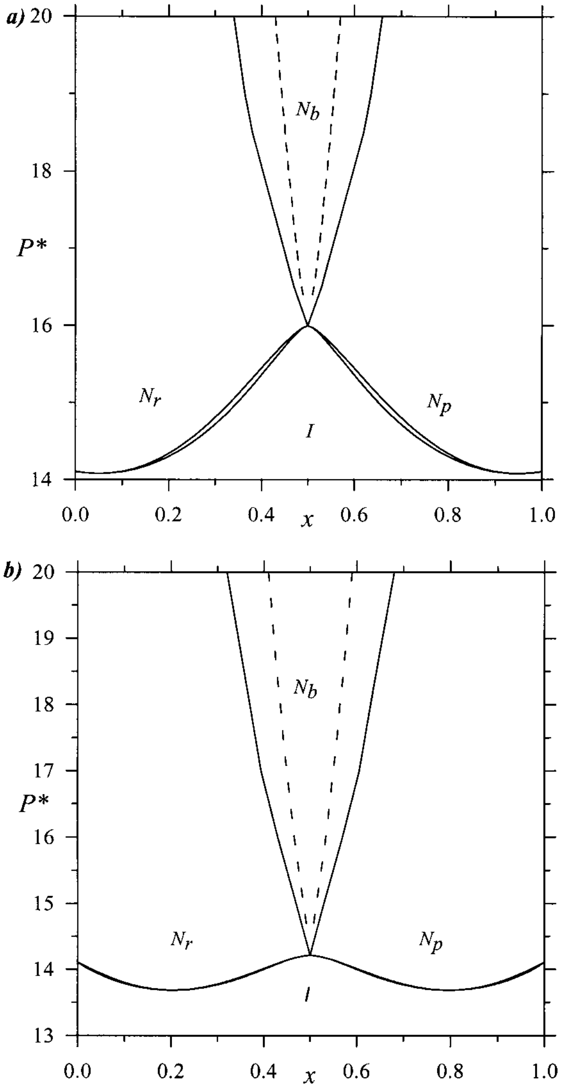

FIG. 8. Pressure-composition (P^*x) representation of the phase diagram of a symmetric rod-plate mixture obtained using a numerical solution for (a) $q=0.5$ and (b) $q=0.6$. The continuous curves represent the stable coexistence curves of the isotropic-nematic and nematic–biaxial nematic transitions, while the dashed curves indicate the metastable nematic-nematic demixing transition. The labels I, N_r, N_p, and N_b denote isotropic, rod-rich nematic, plate-rich nematic, and biaxial nematic phases, respectively. x corresponds to the mole fraction of the plates.

the isotropic-nematic coexistence region, and the region of stability of the biaxial phase are found to be more extensive when determined with the numerical solution. Again one should bear in mind that for these small values of q the Onsager second virial theory will not provide a quantitative description of the system.

The phase diagram obtained with the full numerical approach for $q=0.6$ is very similar to the one obtained using the L2 approximation with the slightly smaller value of $q=0.5$ [see Figs. 3(a) and 8(b)]. The isotropic-nematic first-order transition is very weak in terms of composition difference, but not in density, and two azeotropic points are seen at about $x=0.2$ and 0.8; a stabilization of the isotropic phase relative to the nematic phase is found for compositions between 0.2 and 0.8, while a destabilization is found close to the pure component axes. Note that the phase diagram obtained for $q=0.6$ with the L2 approximation [Fig. 3(b)] is considerably different from that obtained numerically [Fig. 8(b)], the former exhibiting a destabilization of the isotropic phase for the entire composition range. These quantitative differences are the result of the approximation introduced in the solution of the excluded volume integrals in the L2 model (see Fig. 1).

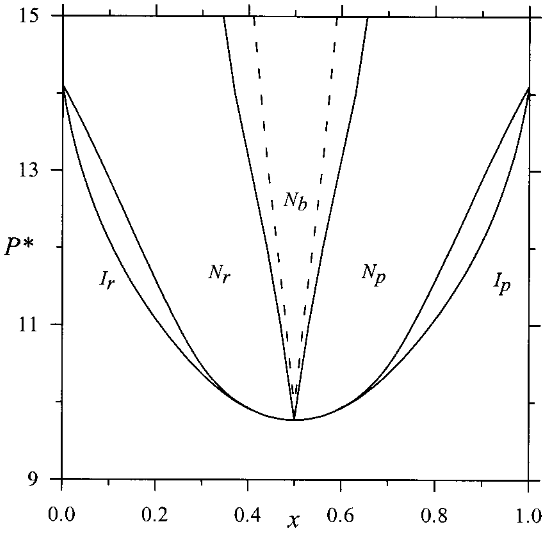

FIG. 9. Pressure-composition (P^*x) representation of the phase diagram of a symmetric rod-plate mixture obtained using a numerical solution for $q=1.0$. The continuous curves represent the stable coexistence curves of isotropic-nematic and nematic–biaxial nematic transitions, while the dashed curves indicate the metastable nematic-nematic demixing transition. The additional labels I_r and I_p denote a rod-rich isotropic phase and a plate-rich isotropic phase, respectively.

We now turn our attention to systems with larger values of the unlike excluded volume parameter q, which correspond to larger aspect ratios for which the Onsager theory is known to be more accurate. The first study of the rod-plate mixture phase diagram using the approach of Onsager was carried out with the L2 approach by Stroobants and Lekkerkerker for the system with $q=1$ [25] ($\kappa=39.5$ and $\kappa'=12.6$). Later, Vanakaras and Photinos [26] reexamined the phase behavior of rod-plate mixtures using a variational approach at the level of the second virial coefficient. For a given choice of molecular parameters, Vanakaras and Photinos reproduce the phase diagram presented by Stroobants and Lekkerkerker with an additional analysis of nematic-nematic demixing. Vanakaras and Photinos concluded that the system does not demix in this case, but demixing of the nematic phase could be found when the form of the unlike excluded volume was changed. It is important to note, however, that in the work of Vanakaras and Photinos, the unlike excluded volume is not given by a $|\cos\gamma|$ function, and is instead determined arbitrarily. For the system with $q=1$, our results (see Fig. 9) are qualitatively similar to those of Stroobants and Lekkerkerker [25] and of Vanakaras and Photinos [26]; different transition

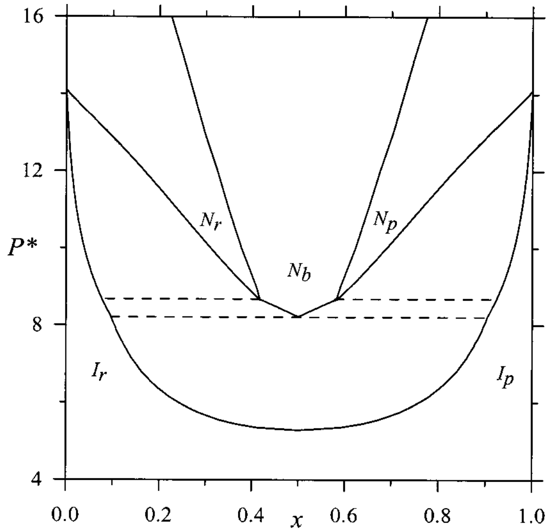

FIG. 10. Pressure-composition (P^*x) representation of the phase diagram of a symmetric rod-plate mixture obtained using a numerical solution for $q=1.6$. The continuous curves represent the stable coexistence curves of isotropic-nematic, nematic–biaxial nematic, isotropic–biaxial nematic, and isotropic-isotropic transitions. The dashed lines indicate the pressures at which three phases are found in coexistence.

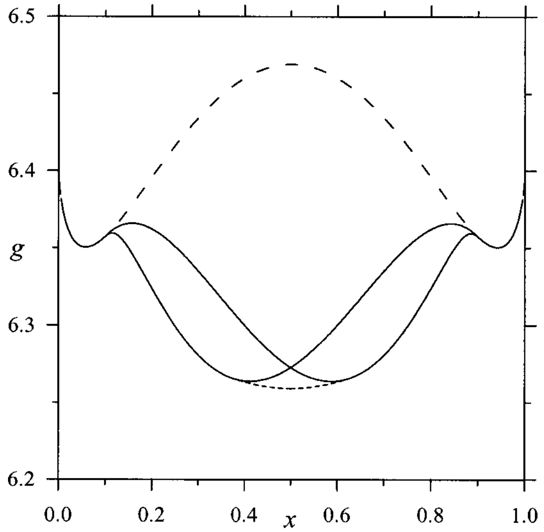

FIG. 11. Gibbs free energy density versus composition for a symmetric mixture of rods and plates obtained using a numerical solution for $q=1.6$ and $P^*=10$. The continuous curves show the rod-rich and plate-rich nematic solutions, while the long- and short-dashed curves correspond to the metastable isotropic and the stable biaxial nematic solutions, respectively.

pressures are obtained when the numerical solution is used, as was mentioned earlier, and the range of biaxial nematic phase is wider in our work, as observed for the lower values of q.

The more interesting mixture with the large value $q=1.6$, for which the biaxial phase was not found in the L2 model [see Fig. 6(b)], is depicted in Fig. 10. It can be seen that the numerical method provides a qualitatively different phase diagram, with an extensive region of biaxial nematic stability, and no nematic-nematic demixing is observed for the pressure range studied. Nematic-nematic demixing may be possible at very high pressures but in this case the numerical solution becomes difficult due to the sharply peaked nature of the orientational distribution functions. Isotropic-isotropic demixing is observed at lower pressures, and in a narrow range of intermediate pressures a region of isotropic–biaxial nematic coexistence is also found, limited above and below by two pressures at which three phases are found in coexistence (biaxial nematic–isotropic–isotropic below, and isotropic–nematic–biaxial nematic above). As before, the region of isotropic-isotropic demixing ends at a minimum pressure critical point. These results are further illustrated in Fig. 11, where the Gibbs free energy at $P^*=10$ is shown. A first-order isotropic-nematic phase transition and a second-order nematic–biaxial nematic transition can be clearly seen. The demixed nematic phases have higher Gibbs free energy than the biaxial nematic phase for all the compositions where they are found.

In summary, we show that, while the phase diagrams obtained using the L2 approximation and the numerical solution are qualitatively equivalent for values of q close to 1, a rather different phase behavior is obtained for $q>1$. The possibility of nematic-nematic phase separation in the numerical approach cannot, however, be excluded. The numerical difficulties encountered at high pressures, together with the appearance of more ordered (smectic and columnar) phases, which are not incorporated in the theory, prevent us from studying higher pressures.

IV. CONCLUSION

In this paper we have studied the phase behavior of a symmetric binary mixture of hard rodlike and platelike molecules using Onsager's second virial theory. We have focused on two important issues: the effect of varying the unlike excluded-volume interaction (characterized by the parameter q), and the accuracy of the commonly used L2 approximation. The simplicity of the L2 method is indisputable, but the poor description of the excluded volume in this case means that it can give rise to a very different phase behavior from that predicted by an exact numerical solution. We show that even after expanding the excluded volume in terms of Legendre polynomials up to 18th order (L18 model) there are inherent errors due to the slow convergence of the series for the parallel and perpendicular configurations; unfortunately, these are particularly important in the biaxial and nematic phases. Other methods, such as those involving trial orientational distribution functions [43], are also reasonably easy to implement but cannot be applied to weakly ordered liquid crystalline phases. The numerical method does not suffer from any of these problems. It is, however, considerably more demanding in terms of computational requirements, and it becomes prohibitive for very aligned phases when the grid of the angle integrals would have to be very small [18].

The richness in phase behavior exhibited by this relatively simple hard-core mixture is highlighted. The stability of the isotropic-nematic transition depends on the value of the parameter q, which results in a stabilization of either the isotropic ($q<0.5$ in the L2 approximation or $q<0.6$ for the numerical solution) or the nematic ($q>0.5$ in the L2 approximation or $q>0.6$ for the numerical solution) phase. The use of the L2 approximation indicates the possibility of stable regions of the biaxial nematic phase for $q<1.5$. Nematic-nematic phase separation occurs at high pressures (densities), eventually preempting the stable biaxial phase altogether. When the numerical solution is employed, no nematic demixing was observed in any of the mixtures studied within the pressure range investigated. This conclusion is in contrast with the results obtained with the L2 solution, and the results of the Mayer-Saupe models [13–15]. Demixing of the isotropic phase is also found (for $q>1.5$ for both the L2 and the numerical solutions), which has not been reported previously for mixtures of rod and plate particles. In addition, an unusual isotropic-biaxial nematic first-order transition is observed with the numerical solution. This transition has been suggested in systems of biaxial particles [50], but here it is observed in a system of uniaxial particles.

Before finishing our discussion, it is important to acknowledge the shortcomings of our approach. The approach of Onsager is accurate only for long rods ($\kappa>20$), and it is always approximate for plates. Extending the approach to shorter and more realistic aspect ratios of the rod particles (taking into account the shape of the particle and end effects) can be achieved by appropriate resummation of higher virial terms [36,37]. An improvement of the predictions for the phase behavior of platelike molecules is, however, more demanding. It has been shown that the inclusion of higher virial terms (up to the fifth virial coefficient) does not improve the results substantially for infinitely thin plates [4]. However, a recent comparison of the resummed Onsager theory (using the scaling of Parsons) with simulation data for platelike cutspheres [51] indicates that the theory can give accurate results for moderate aspect ratios. In future work we plan to examine the phase diagram of a rod-plate mixture using a Parsons resummation of the Onsager theory to compare it with the simulation data, and to examine the effect of the lower order terms (end effects) of the excluded volumes on the competition of nematic-nematic and nematic–biaxial nematic transitions.

ACKNOWLEDGMENTS

S.V. would like to thank the ROPA program (GK/N03358) of the Engineering and Physical Sciences Research Council (EPSRC) for support and A.G. would like to thank the EPSRC for support. We acknowledge support from the Joint Research Equipment Initiative (JREI) of the EPSRC for computer hardware (GR/M94427), and the Royal Society-Wolfson Foundation for the award of a refurbishment grant.

---

[1] L. Onsager, Ann. N.Y. Acad. Sci. **51**, 627 (1949).
[2] J. Vieillard-Baron, J. Chem. Phys. **56**, 4729 (1972).
[3] D. Frenkel, J. Phys. Chem. **92**, 3280 (1988); D. Frenkel, H. N. W. Lekkerkerker, and A. Stroobants, Nature (London) **332**, 822 (1988).
[4] R. Eppenga and D. Frenkel, Mol. Phys. **52**, 1303 (1984).
[5] P. G. de Gennes, *The Physics of Liquid Crystals*, 2nd ed. (Clarendon, Oxford, UK, 1996).
[6] P. J. Camp and M. P. Allen, J. Chem. Phys. **106**, 6681 (1997).
[7] J. A. C. Veerman and D. Frenkel, Phys. Rev. A **45**, 5632 (1992).
[8] R. Blaak, D. Frenkel, and B. M. Mulder, J. Chem. Phys. **110**, 11 652 (1999).
[9] R. Alben, J. Chem. Phys. **59**, 4299 (1973).
[10] R. van Roij and B. M. Mulder, J. Phys. II **4**, 1763 (1994).
[11] E. Sokolova and A. Vlasov, J. Phys.: Condens. Matter **9**, 4089 (1997).
[12] E. P. Sokolova, I. K. Tokhadze, and N. A. Smirnova, Russ. J. Phys. Chem. **75**, 1319 (2001).
[13] P. Palffy-Muhoray, J. R. de Bruyn, and D. A. Dunmur, Mol. Cryst. Liq. Cryst. **127**, 301 (1985).
[14] P. Palffy-Muhoray, J. R. de Bruyn, and D. A. Dunmur, J. Chem. Phys. **82**, 5294 (1985).
[15] S. R. Sharma, P. Palffy-Muhoray, B. Bergersen, and D. A. Dunmur, Phys. Rev. A **32**, 3752 (1985).
[16] T. M. Birshtein, B. I. Kogelov, and V. A. Pruamitsyn, Polym. Sci. U.S.S.R. **30**, 316 (1988).
[17] G. J. Vroege and H. N. W. Lekkerkerker, J. Phys. Chem. **97**, 3601 (1993).
[18] S. Varga and I. Szalai, PCCP **2**, 1955 (2000).
[19] R. van Roij, B. M. Mulder, and M. Dijkstra, Physica A **261**, 347 (1998).
[20] R. P. Sear and B. M. Mulder, J. Chem. Phys. **105**, 7727 (1996).
[21] R. P. Sear and G. Jackson, J. Chem. Phys. **103**, 8684 (1995).
[22] P. C. Hemmer, Mol. Phys. **96**, 1153 (1999).
[23] P. C. Hemmer, J. Stat. Phys. **100**, 3 (2000).
[24] Z. Y. Chen and J. M. Deutch, J. Chem. Phys. **80**, 2151 (1984).
[25] A. Stroobants and H. N. W. Lekkerkerker, J. Phys. Chem. **88**, 3669 (1984).
[26] A. G. Vanakaras and D. J. Photinos, Mol. Cryst. Liq. Cryst. **299**, 65 (1997).
[27] A. G. Vanakaras, S. C. McGrother, G. Jackson, and D. J. Photinos, Mol. Cryst. Liq. Cryst. **323**, 199 (1998).
[28] A. G. Vanakaras, A. F. Terzis, and D. J. Photinos, Mol. Cryst. Liq. Cryst. **362**, 67 (2000).
[29] E. P. Sokolova, N. A. Smirnova, and I. K. Tokhadze, Russ. J. Phys. Chem. **74**, S357 (2000).
[30] R. E. Goozner and M. M. Labes, Mol. Cryst. Liq. Cryst. **56**, 75 (1979).
[31] F. Hardouin, G. Sigaud, M. F. Achard, and H. Gasparaux, Mol. Cryst. Liq. Cryst. **58**, 155 (1979).
[32] L. J. Yu and A. Saupe, Phys. Rev. Lett. **45**, 1000 (1980).
[33] F. M. van der Kooij and H. N. W. Lekkerkerker, Langmuir **16**, 10144 (2000).
[34] F. M. van der Krooij and H. N. W. Lekkerkerker, Phys. Rev. Lett. **84**, 781 (2000).
[35] H. H. Wensink, G. J. Vroege, and H. N. W. Lekkerkerker, J. Chem. Phys. **115**, 7319 (2001).

[36] J. D. Parsons, Phys. Rev. A **19**, 1225 (1979).
[37] S. D. Lee, J. Chem. Phys. **87**, 4972 (1987).
[38] P. J. Camp and M. P. Allen, Physica A **229**, 410 (1996).
[39] P. J. Camp, M. P. Allen, P. G. Bolhuis, and D. Frenkel, J. Chem. Phys. **106**, 9270 (1997).
[40] A. Galindo, G. Jackson, and D. J. Photinos, Chem. Phys. Lett. **325**, 631 (2000).
[41] A. Chrzanowska, Phys. Rev. E **58**, 3229 (1998).
[42] R. Zwanzig, J. Chem. Phys. **39**, 1714 (1963).
[43] G. J. Vroege and H. N. W. Lekkerkerker, Rep. Prog. Phys. **55**, 1241 (1992).
[44] J. S. Rowlinson and F. L. Swinton, *Liquids and Liquid Mixtures*, 3rd ed. (Butterworth Scientific, London, 1982).
[45] C. G. Gray and K. E. Gubbins, *Theory of Molecular Liquids* (Clarendon, Oxford, 1984), Vol. 1, Fundamentals.
[46] S. D. P. Flapper and G. Vertogen, Phys. Rev. A **24**, 2089 (1981).
[47] W. H. Press, B. P. Flannery, S. A. Teukolsky, and W. T. Vetterling, *Numerical Recipes in Fortran*, 1st ed. (Cambridge University Press, London, 1986).
[48] S. Varga, A. Galindo, and G. Jackson (unpublished).
[49] R. F. Kayser and H. J. Ravaché, Phys. Rev. A **17**, 2067 (1978).
[50] B. M. Mulder, Phys. Rev. A **39**, 360 (1989).
[51] S. Varga, A. Galindo, and G. Jackson (unpublished).